Influence of anisotropy and pinning centers on critical current properties in Bi-2212 superconductors

T. Haraguchi [a], S. Takayama [a], M. Kiuchi [a], E. S. Otabe [a], T. Matsushita [a,1], T. Yasuda [a], S. Okayasu [b], S. Uchida [c], J. Shimoyama [c], K .Kishio [c],

[a] *Department of Computer Science and Systems Engineering, Kyushu Institute of Technology, 680–4 Kawazu, Iizuka 820–8502, Japan*

[b] *Japan Atomic Energy Agency, 2–4 Shirane, Tokai-mura, Naka-gun, Ibaraki, 319–1195, Japan*

[c] *Department of Superconductivity, University of Tokyo, 7–3–1, Hongo, Bunkyo-ku, Tokyo, 113–8656, Japan*

Abstract

The critical current density in Bi-2212 superconductors with various anisotropies irradiated by heavy ions was investigated in the medium temperature region to understand the effects of defect size and the anisotropy of the superconductor. It was found that the critical current density and the irreversibility field were larger for the specimen with larger defect and/or with smaller anisotropy. Introduction of stronger pinning centers and the optimization of the doping condition to improve the

Preprint submitted to PCP–55/ ISS2005 *Submitted 25 October 2005*

dimensionality are desired for further improvement of the critical current properties.

Keywords: Bi-2212 superconductor, columnar defect, anisotropy parameter,

irreversibility field,

PACS: 75.30.Gw

---

1 Introduction

It is known that Bi-2212 superconductor has a very high critical current density up to high fields at low temperatures. This is attributed to the high condensation energy density at low temperatures [1]. Therefore, various applications of this superconductor is expected, such as a power generator, a magnet for superconducting magnetic energy storage, *etc.* The introduction of suitable pinning centers is desired for further improvement of the pinning properties at low temperatures. On the other hand, the pinning properties are poor at high temperatures due to a significant reduction in the condensation energy density. This is an inevitable nature of the two-dimensional supercon-

[1] Corresponding author: T. Matsushita

Postal address: Department of Computer Science and Electronics, Kyushu Institute of Technology, 680-4, Kawazu, Iizuka 820–8502 Japan

Phone: +81–948–29–7663

Fax: +81–948–29–7661

E-mail address: matusita@cse.kyutech.ac.jp (T. Matsushita)

ductivity with thick and almost insulating block layers.

Thus, the next interest is the possibility of improvement of the critical current density of Bi-2212 superconductors in the medium temperature region. For this purpose it is desirable to increase the dimensionality of the superconductor by oxygen doping or by Pb doping, since these improve the superconductivity in the block layers. The introduction of strong pinning centers is also important. As was previously reported, the columnar defects with radius larger than the coherence length are effective to realize a high pinning performance. In fact, the critical current density of 1.4×10^9 A/m^2 was obtained at 20 K and at 2 T even for a specimen with a low density of columnar defect with radius of about 5.0 nm [2].

In this paper, the flux pinning properties of Bi-2212 superconductor in the medium temperature region is examined. To understand the mechanism which determines the critical current density, the flux pinning by columnar defects is chosen, and the effects of defect size and the anisotropy parameter on the critical current density and the irreversibility field are investigated.

2 Experimental

2.1 Specimens

Specimens used in this study were Bi-2212 single crystals. Specimens A $\sim$ D were prepared by the floating-zone method, and the typical size of the specimens was 2 mm $\times$ 1 mm $\times$ 10 μm. These specimens were irradiated by iodine ions with acceleration energy of 200 MeV along the c-axis. Specimens #1 $\sim$ #3 were prepared by the KCl flux method, and the typical size of the specimens were 2 mm $\times$ 1.5 mm $\times$ 7 μm. These were irradiated by nickel ions with acceleration energy of 180 MeV in the same direction. The matching field for dose, B_ϕ, was 1.0 T for all the specimens. The radius of columnar defects was about 5.0 nm(iodine ions) and 2.0 nm(nickel ions), respectively. Specifications of specimens are listed in Table 1.

2.2 Measurement

A DC magnetization was measured using a SQUID magnetometer in a magnetic field parallel to the c-axis. The critical current density J_c is estimated from a width of magnetization hysteresis, ΔM, as

$$J_\mathrm{c} = \frac{6a}{b(3a-b)}\Delta M \qquad (1)$$

with an assumption of Bean's model. Here, a and b are the width and the length of the specimen($a > b$), respectively. The irreversibility field $B_{\rm i}$ is determined by the magnetic field at which $J_{\rm c}$ reduces to 1.0×10^7 A/m^2.

The anisotropy parameter $\gamma_{\rm a}$ is estimated from $\gamma_{\rm a}^2 = \phi_0/B_{\rm p}s^2$ [3] at $T/T_{\rm c} = 0.25$ for a consistency with the previous work [2], where $B_{\rm p}$ is a peak field, ϕ_0 is a flux quantum and $s(\simeq 1.5$ nm) is a distance between the superconducting layers.

3 Theory

According to the flux creep-flow theory [4], the current-voltage curve of a superconductor under a flux creep is determined by the pinning potential, U_0, for a flux bundle:

$$U_0 = \frac{0.835 k_{\rm B} g^2 J_{\rm c0}^{1/2}}{\zeta^{3/2} B^{1/4}}, \tag{2}$$

where $k_{\rm B}$ is the Boltzmann constant, g^2 is a number of flux lines in the flux bundle and $J_{\rm c0}$ is the virtual critical current density in the flux-creep free case. ζ is a constant depending on the kind of pinning center, and $\zeta = 4$ is known for strong pinning centers. The temperature and magnetic field dependence of $J_{\rm c0}$ is assumed as

$$J_{\rm c0} = A(T)(B + B_0)^{\gamma-1}\left(1 - \frac{B}{B_{\rm c2}}\right)^2, \tag{3}$$

where $A(T)$ is temperature dependent parameter describing the flux pinning strength, and B_0 and γ are the pinning parameters. Here it is assumed that the temperature dependence of $A(T)$ is expressed as

$$A(T) = A_0 \left(1 - \frac{T}{T_c}\right)^m . \tag{4}$$

A nonuniform spatial distribution of columnar defects is approximated by the statistical distribution of A_0 as

$$f(A_0) = K \exp\left[-\frac{(\log A_0 - \log A_{0\mathrm{m}})^2}{2\sigma^2}\right], \tag{5}$$

where $A_{0\mathrm{m}}$ is a most probable value of A_0, σ^2 is a parameter representing a distribution width and K is a normalization constant. The local electric field, E', is determined from the mechanism of flux creep and flow, and can be expressed using Eq. (2) for a given value of J. Thus, the average E-J curve is calculated from

$$E(J) = \int_0^\infty E' f(A) \mathrm{d}A. \tag{6}$$

The details of the analysis are described in [4]. The theoretical J_c-value is determined from the calculated E-J curve with the electric field criterion of 2.0×10^{-8} V/m of the same condition in the experiment. The pinning parameters, $A_{0\mathrm{m}}$, m, B_0 and γ were determined so as to obtain a good agreement between theoretical and experimental results of J_c at each temperature. $\sigma^2 = 0.001$ and $g^2 = 1$ are used in the theoretical calculation. Other pinning parameters are listed in Table 2.

4 Results and Discussion

Figure 1 shows the magnetic field dependence of the critical current density for specimen D. In this figure, open and solid symbols are the experimental results. It is found that a plateau appears at around $B_\phi/3$ and at $T = 55 \sim 60$ K. The solid lines are the theoretical results of the critical current density. These were fitted to the experimental results in the magnetic field region sufficiently higher than $B_\phi/3$, since the pinning properties above $B_\phi/3$ were considered to be quite different from those below $B_\phi/3$. A good agreement is obtained between the theoretical and experimental results in such higher magnetic fields.

Figure 2 shows the temperature dependence of the irreversibility field of the specimens after the irradiation by (a) iodine ions and (b) nickel ions, where solid symbols are experimental values and open symbols are theoretical values. The solid and dotted lines are guides for eyes. The irreversibility field increases with decreasing temperature and a plateau appears at around $T/T_\mathrm{c} \simeq 0.5$. The increase becomes very steep below $T/T_\mathrm{c} = 0.3$ due to the crossover of flux lines into the two dimensional state. However, the flux lines are forced to be in the quasi-three-dimensional state due to the strong interaction with the parallel columnar defects [2]. It is found that the irreversibility field is higher for the specimen with the lower anisotropy parameter. In addition, it is found that the irreversibility field is higher for the specimen irradiated by iodine ions. This is due to the effect of defect size. That is, the defects of larger size have a higher probability to encounter the flux lines, giving rise to a stronger pinning [5].

Figure 3 shows the dependence of the experimental irreversibility field at $T/T_{\rm c} = 0.6$ on the anisotropy parameter. The irreversibility field increases with decreasing anisotropy parameter. This comes from the difference in the condensation energy density. The experimental results are divided into two groups with different defect sizes as discussed above. The irreversible field of the specimens with larger defects is about 3 times as large as that of specimens with smaller defects.

Figures 4 (a) and 4(b) show the relationship between the condensation energy density and the flux pinning strength given by

$$A_{\rm m}(T) = A_{0{\rm m}} \left(1 - \frac{T}{T_{\rm c}}\right)^{m} \tag{7}$$

at $T/T_{\rm c} = 0.3$ and $T/T_{\rm c} = 0.6$, respectively. At $T/T_{\rm c} = 0.3$, the pinning strength is approximately proportional to the condensation energy density: the exponent shown by the lines in Fig. 4(a) is 1.2. This suggests that the linear summation of the flux pinning forces with a high pinning efficiency holds approximately at low temperatures due to relative strong pinning of the columnar defects, since the elementary pinning force of each columnar defect is proportional to the condensation energy density. On the other hand, the condensation energy density becomes small at high temperatures, resulting in a weaker pinning. It is considered that the pinning mechanism is changing from the linear summation to the statistical summation with increasing temperature. In the statistical summation regime the pinning strength is proportional to the second power of the elementary pinning force with a low pinning efficiency. In Fig. 4(b) the exponent shown by the lines is 1.5.

In Figs. 4(a) and 4(b), it is also found that the results are divided into two groups similarly to the result on the irreversibility field. That is, the flux pinning is stronger for the specimen with larger defects. According to the theoretical prediction [6], the irreversibility field is approximately proportional to $A_{\mathrm{m}}^{1/3}(T)$, when B_{c2} is sufficiently higher than B_{i}. Hence, the difference of a factor of 40 observed in $A_{\mathrm{m}}(T)$ for the two groups approximately explains the difference of the irreversibility field of the above factor of about 3 ($40^{1/3} \simeq 3.4$) due to the difference of the defect size.

It was found that the superconducting property strongly depends on both the dimensionality of the superconductor and the size of defects. This means that the more three-dimensional superconductivity is desired. For this purpose it is necessary to investigate the optimum condition of O_2 doping or Pb doping. As for the pinning, larger columnar defects have lower pinning efficiencies, although those have stronger pinning forces. Hence, the optimization of the defect size is important. Furthermore, the pinning property of the columnar defects is rather poor in spite of the large elementary pinning force, since the probability of pinning flux lines by parallel columnar defects is low. Therefore, the shape of pinning centers is also important. It is considered that the introduction of planar pinning centers with higher pinning efficiencies is effective for further improvement of characteristics in the future.

5 Summary

The flux pinning properties in Bi-2212 superconductor in the medium temperature region was examined and the effects of defect size and the anisotropy parameter on the critical current density and the irreversibility field were investigated. As a result, the critical current density and the irreversibility field were larger for the specimen with smaller anisotropy and/or with larger defects. Therefore, these are key factors which determine the applicability of Bi-2212 superconductors. It is important to enhance the dimensionality of the superconductor for improvement of the characteristics especially at low temperatures. For this purpose, it is necessary to investigate the optimum doping condition to improve the dimensionality. For practical applications especially at high temperatures, the introduction of stronger pinning centers than in the present work is desired, since the pinning efficiency becomes lower at higher temperatures. Therefore, the optimization of size and morphology of pinning centers is needed.

References

[1] T. Matsushita, K. Okamura, M. Kiuchi, E. S. Otabe, T. Yasuda, S. Okayasu, Adv. Cryog. Eng. Mater. 50B (2004) 627.

[2] K. Okamura, M. Kiuchi, E. S. Otabe, T. Yasuda, T. Matsushita, S. Okayasu, S. Uchida, J. Shimoyama, K. Kishio, Physica C 412-414 (2004) 416.

[3] V. M. Vinokur, P. H. Kes, A. E. Koshelev, Physica C 168 (1990) 29.

[4] M. Kiuchi, K. Noguchi, T. Matsushita, T. Kato, T. Hikata, K. Sato, Physica C 278 (1997) 62–70.

[5] T. Matsushita, M. Kiuchi, T. Haraguchi, T. Imada, E. S. Otabe, T. Yasuda, K. Okamura, S. Okayasu, S. Uchida, J. Shimoyama, K. Kishio, to be published.

[6] N. Ihara, T. Matsushita, Physica C 257 (1996) 223.

Table 1: Specification of specimens.

specimen	condition of oxygen doping	T_c(K)	size(mm)	thickness(μm)	γ_a
A	$\sim$ 700℃, 0.1MPa(air)	87.0	1.82×2.04	13	187
B	500℃, 0.1MPa(air)	88.9	0.72×1.60	11	148
C	400℃, 0.09MPa(O_2)	84.6	0.99×2.09	11	127
D	400℃, 0.21MPa(O_2)	78.4	0.92×2.12	8	93
#1	400℃, 26.6Pa(air)	88	1.78×1.18	5	132
#2	550℃, 0.1MPa(air)	87	2.07×1.65	9	111
#3	400℃, 0.1MPa(air)	79	2.24×1.48	6	98

Table 2: Pinning parameters used in theoretical calculation.

specimen	A_{0m}(AT$^{\gamma-1}$/m^2)	m	γ(20K/40K/60K)	B_0(20K/40K/60K)(T)
A	3.2×10^{13}	15.1	$-5.0/-7.0/-0.5$	0.8/1.0/0.03
B	2.8×10^{14}	13.7	$-5.5/-5.5/-2.0$	1.0/0.8/0.4
C	3.3×10^{13}	8.9	$-5.5/-6.5/-2.5$	1.0/1.0/0.6
D	2.1×10^{13}	7.5	$-5.0/-4.5/0$	1.0/1.0/0.03
#1	1.2×10^{12}	13.7	$-2.7/-5.5/-0.6$	0.6/0.8/0.1
#2	3.6×10^{11}	8.8	$-1.5/-4.0/-1.2$	0.5/0.8/0.03
#3	6.2×10^{11}	8.7	$-2.0/-2.0/-0.3$	0.7/0.7/0.1

Figure Captions

Figure 1 Magnetic field dependence of critical current density in specimen D.

Figure 2 Temperature dependence of irreversibility field with (a) iodine ions irradiation and (b) nickel ions irradiation.

Figure 3 Anisotropy parameter dependence of irreversibility field at $T/T_{\rm c} = 0.6$.

Figure 4 Relationship between condensation energy density dependence and flux pinning strength (a) at $T/T_{\rm c} = 0.3$ and (b) at $T/T_{\rm c} = 0.6$.

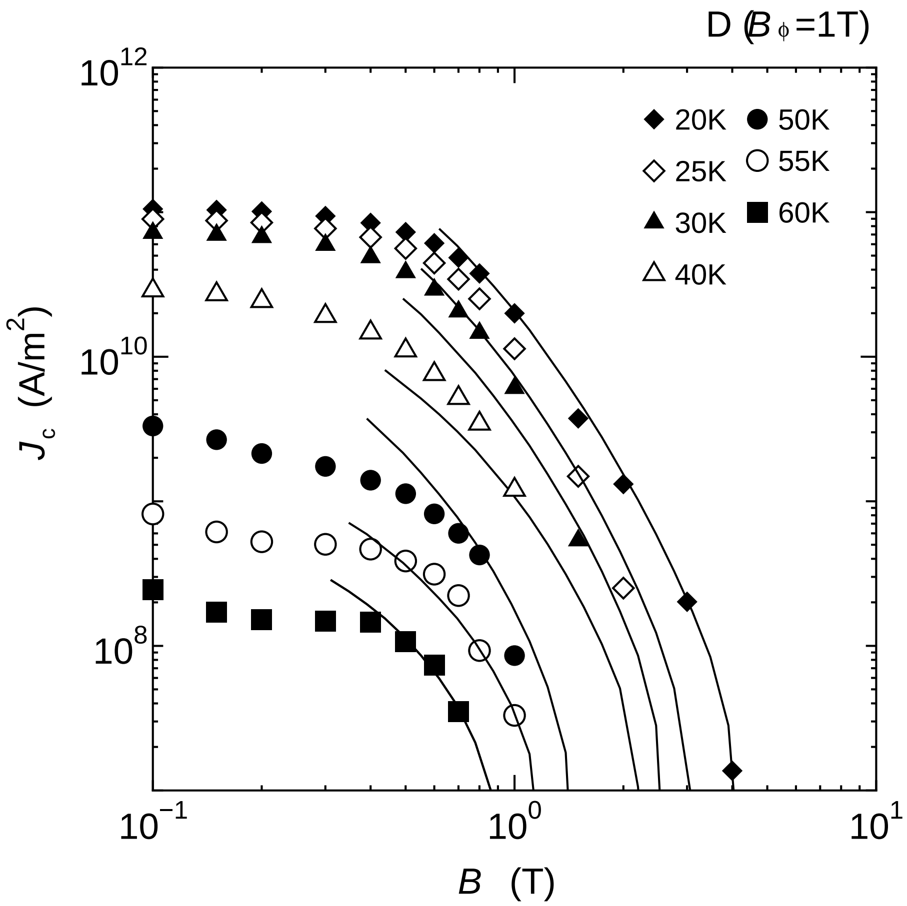

Figure 1: T. Haraguchi *et al.* PCP–55/ ISS2005

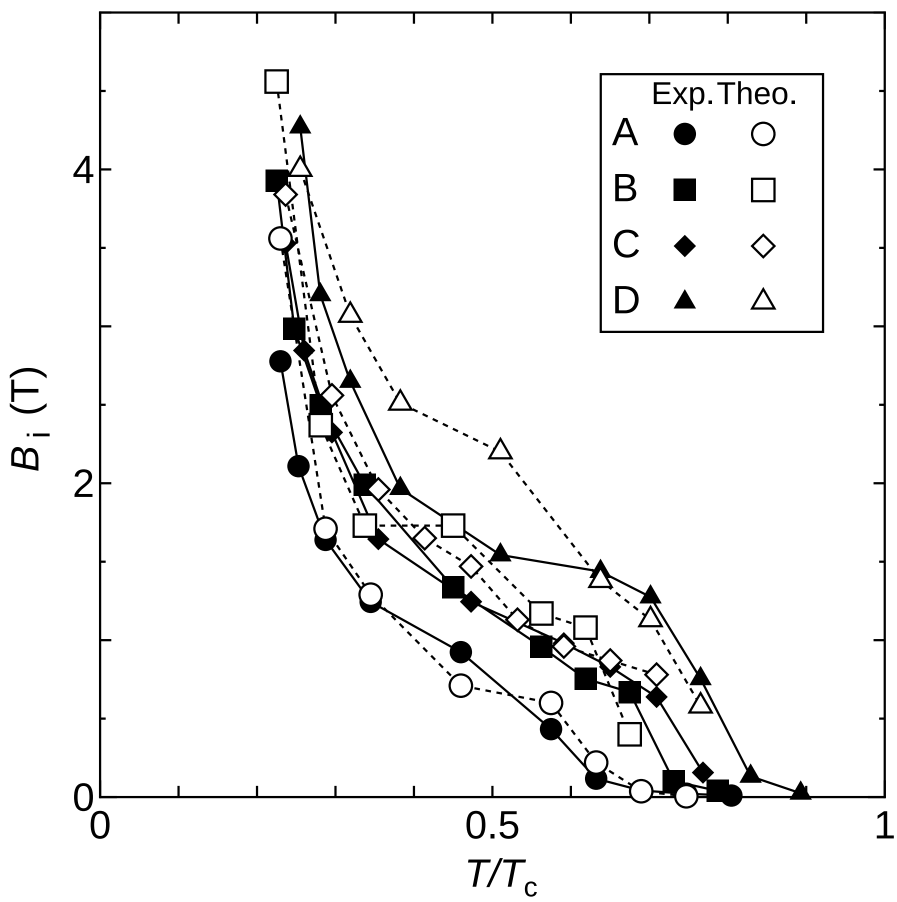

Figure 2(a): T. Haraguchi *et al.* PCP–55/ ISS2005

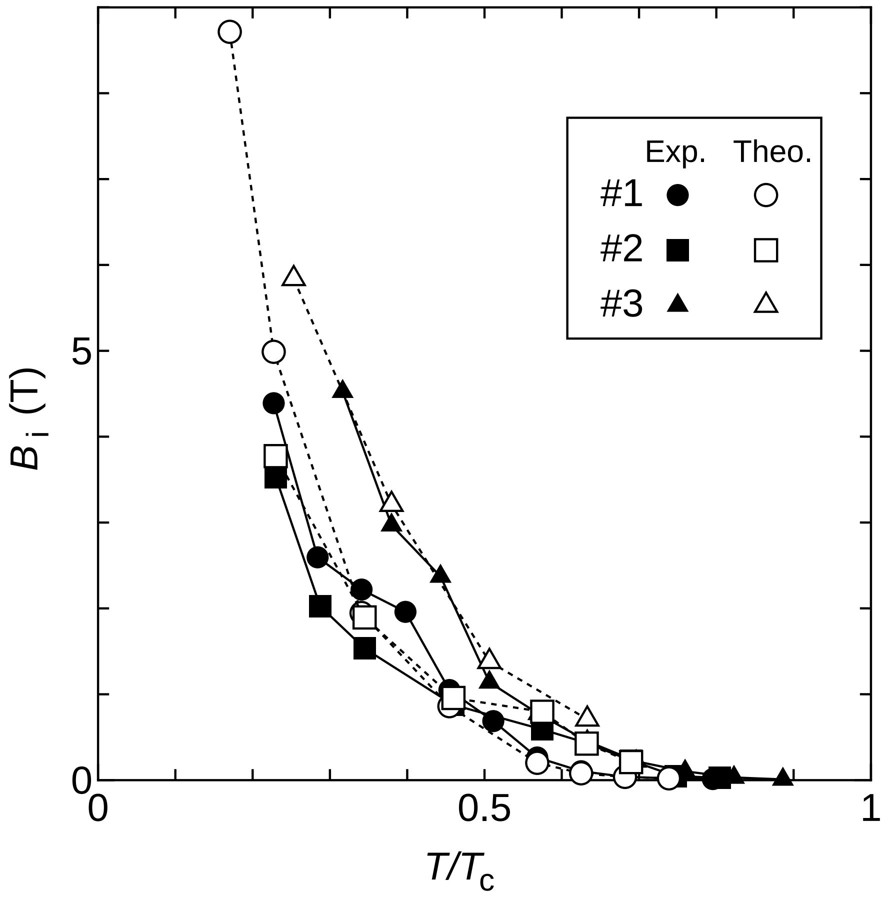

Figure 2(b): T. Haraguchi *et al.* PCP–55/ ISS2005

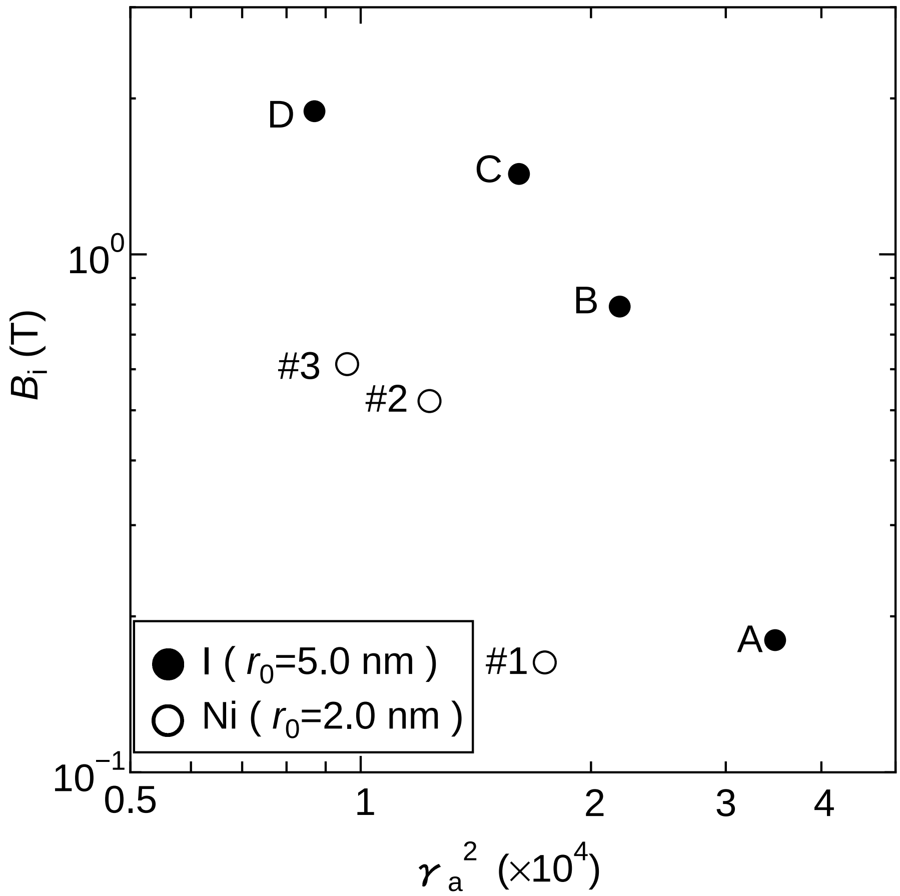

Figure 3: T. Haraguchi *et al.* PCP–55/ ISS2005

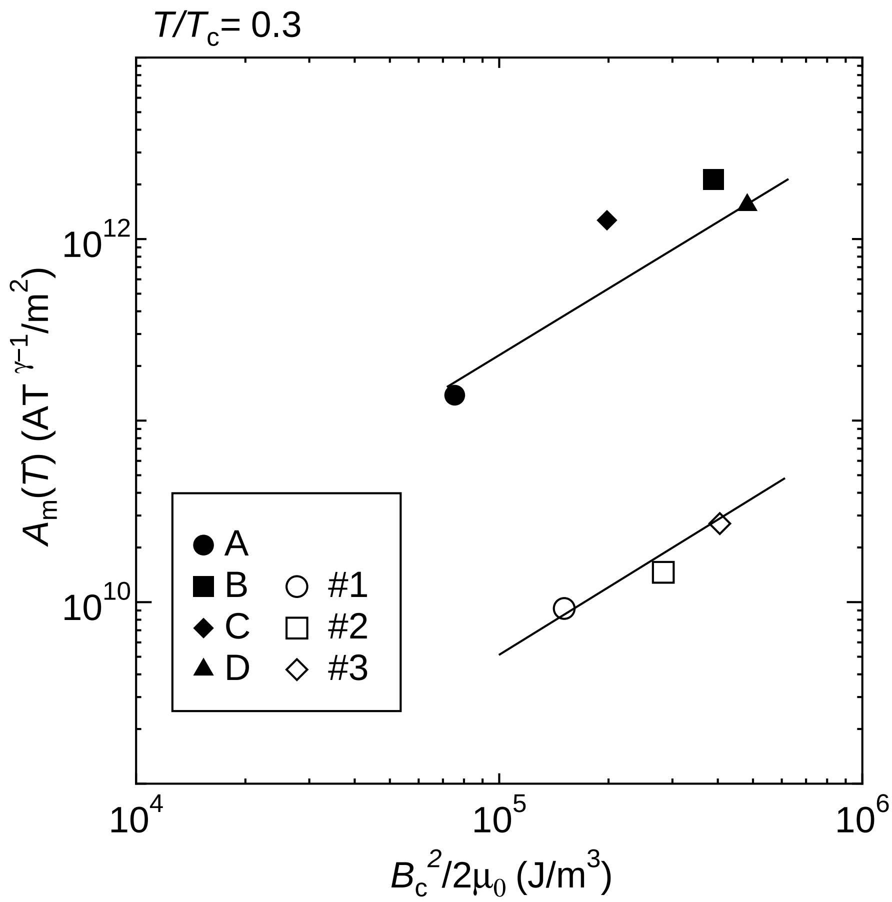

Figure 4(a): T. Haraguchi *et al.* PCP–55/ ISS2005

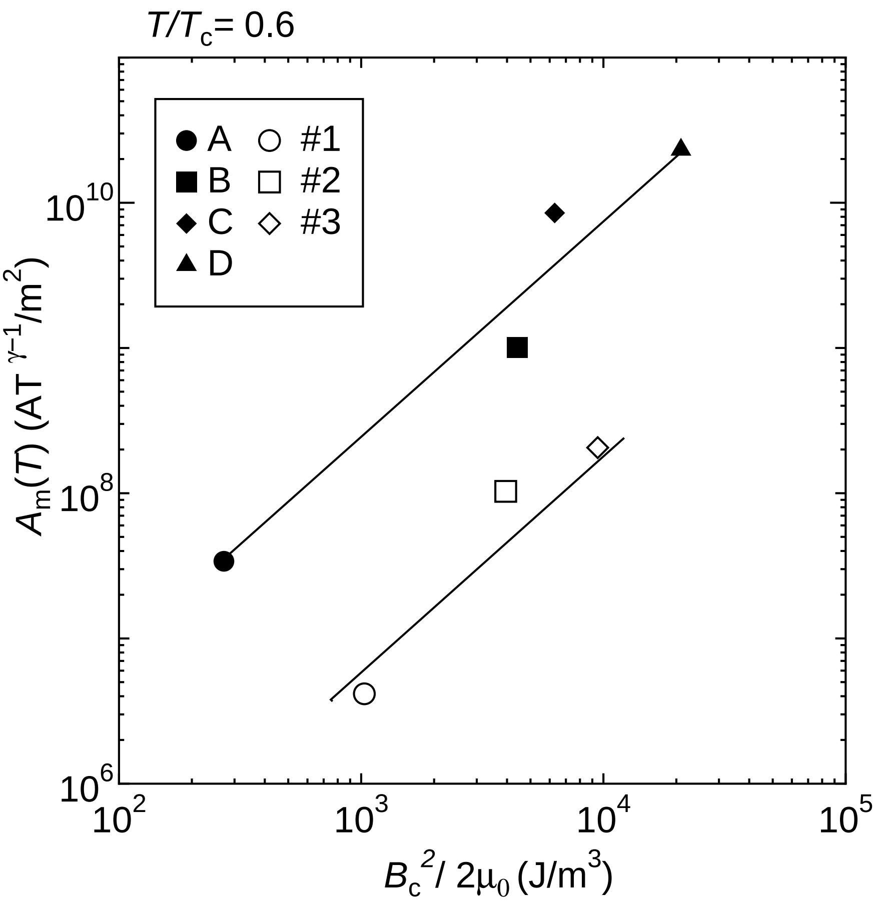

Figure 4(b): T. Haraguchi *et al.* PCP–55/ ISS2005